

Measurements of Gain for Slow Cyclotron Waves on an Annular Electron Beam

H. Guo, L. Chen, H. Keren,^(a) and J. L. Hirshfield
Applied Physics Section, Yale University, New Haven, Connecticut 06520

and

S. Y. Park^(b) and K. R. Chu
Naval Research Laboratory, Washington, D. C. 20375
 (Received 1 June 1982)

Gain was measured for fast and slow waves propagating in a dielectric-loaded TE_{01} axisymmetric waveguide penetrated by an annular electron beam. This measurement is the first reported in the slow-wave regime, where axial velocity modulation dominates the azimuthal bunching. Small-signal gain at 6.0 GHz of over 30 dB, instantaneous bandwidth of 3.7%, and tuning bandwidth of over 11% are reported. In a feedback-amplifier configuration gain of 53 dB, power output of 20 kW, and 10% electronic efficiency are also reported.

PACS numbers: 41.70.+t, 52.35.Hr, 85.10.Hy

Considerable effort over the past decade has been directed towards understanding the convective instability for fast cyclotron waves interacting with electrons on orderly helical orbits in a uniform magnetic field.¹ This interaction is fundamental to the design of novel millimeter-wave gyrotron amplifiers.² The physical mechanism responsible for electromagnetic gain for this system originates with relativistic mass variations with energy which give rise to azimuthal phase bunching for orbiting electrons.³ A competing physical mechanism, originating with axial velocity modulations, tends to oppose the azimuthal phase bunching, but the former mechanism dominates the latter so long as the wave's phase velocity exceeds the light velocity. These mechanisms have been carefully examined and contrasted by Chu and Hirshfield.⁴

For waves with phase velocity below the light velocity, the two mechanisms interchange their roles and the mechanism due to axial velocity modulation dominates the electromagnetic growth. This paper reports results of the first experiment deliberately designed to demonstrate this gain mechanism for slow electromagnetic waves. In fact, both slow and fast waves could be studied on the apparatus and their properties compared. The slow-wave mechanism has the potential for allowing wide-bandwidth operation,⁵ a property not shared by the fast-wave interaction. However, a tapered-structure/tapered-field variant based on the fast-wave mechanism has shown a bandwidth of 13% at 35 GHz⁶; gain is limited to about 20 dB for these fast-wave devices because of the need to use signal injection at the output in order to access the amplifying region in the

device.

The apparatus built to study the slow-wave interaction is shown schematically in Fig. 1. The electromagnetic wave was guided by an axisymmetric structure consisting of a precision-bore Pyrex tube (interior diameter 3.10 cm; wall thickness, 0.20 cm), surrounded by a high-permittivity dielectric annulus (thickness, 0.29 cm), in turn surrounded by a helix waveguide formed by a closely spaced winding of No. 34 AWG copper wire. The helix waveguide was used to suppress lower modes, such as TE_{11} . At one end this composite waveguide tapered out gradually

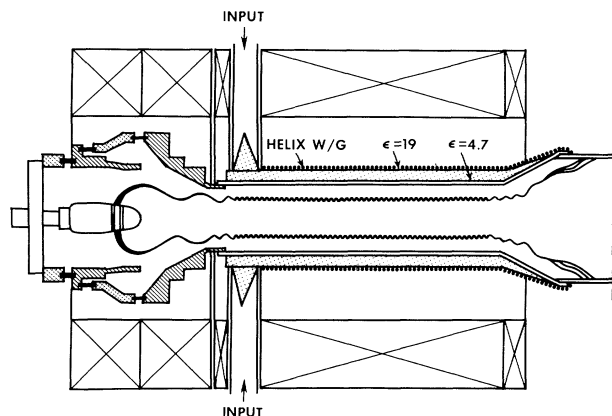


FIG. 1. Schematic outline of experimental configuration (not to scale). Magnetron injection gun at left generated annular electron beam (wiggly lines) which penetrated dielectric-loaded TE_{01} circular waveguide with 60-cm uniform length. The Pyrex tube ($\epsilon = 4.7$) is surrounded by a dielectric layer ($\epsilon = 19$), which in turn is surrounded by a fine-pitch helical winding of No. 34 AWG copper wire.

to a cylindrical copper waveguide of radius 3.7 cm. A mica vacuum window sealed with a gold O ring provided reflection-free output coupling, and a Marié coupler provided output conversion from TE_{01} circular mode to TE_{10} rectangular mode. The Pyrex tube was coated on its interior with a thin carbon film (deposited from a dilute Alkadag solution) to drain off intercepted electron charge. The dc resistance of the film along the entire tube length was about 2 M Ω . The film was scraped off in thin axial stripes to minimize attenuation for the TE_{01} circular mode (TE_{mn} and TM modes were heavily attenuated). Microwave input signals (5–8 GHz) could be injected in the output guide or by means of a two-port coupler (shown in Fig. 1), with ports driven 180° out of phase to allow selective coupling to the TE_{01} mode. Dielectric pyramids were used to aid in coupling into the dielectric layer. Even so, the cold input coupling loss was about 10 dB, and the cold tube insertion loss was also about 10 dB.

The measured dispersion characteristic for this dielectric-loaded waveguide is shown by the heavy curve in Fig. 2(a); it is indistinguishable from the calculated curve. Mode filters were used to insure that TE_{01} was the only propagating mode, both in cold and hot operation. The dispersion curve was obtained by inserting a thin metal foil cylinder between the Pyrex and the dielectric annuli; this foil acted as a movable short circuit allowing measurement of the guide wavelength at each frequency.

The annular electron beam was injected along the dielectric-loaded waveguide from a magnetron injection gun. This gun, procured from an industrial manufacturer,⁷ was built to operate at 60 kV, 5 A, 10^{-3} duty cycle under which conditions it was designed to produce a beam of mean radius 0.95 cm, annular thickness 0.75 cm, $\alpha = v_{\perp}/v_{\parallel} = 2.0$, and relative (rms) parallel velocity spread of 5%. As shall be seen, the gun operating conditions under which the data shown in this paper were obtained were different from the specified values. The gun was driven with ~ 5 - μ sec pulses at 100 sec^{-1} derived from a MIT model 9 modulator⁸ feeding a 4:1 step-up pulse transformer. The gun's intermediate anode voltage was derived from the cathode voltage with a resistive voltage divider, and operated typically between 40% and 60% of cathode voltage. The beam collector was insulated, so that cathode current and transmitted current could be continuously monitored; for the data to be presented here the two were indistinguishable. Cathode cur-

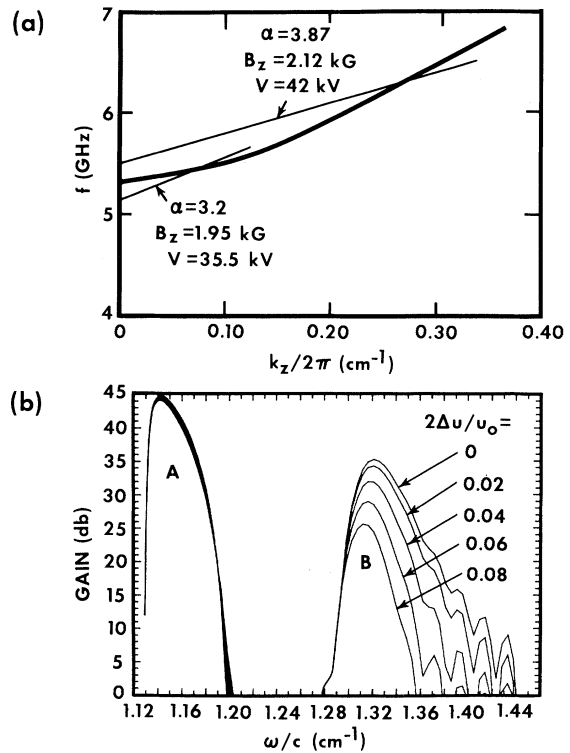


FIG. 2. (a) Measured dispersion curve (heavy line) and typical beam lines $\omega = \Omega/\gamma + k_z u$ for fast- and slow-wave couplings. (b) Calculated gain characteristics in the fast-wave (A) and slow-wave (B) regimes, for five values of parallel velocity spread $2\Delta u/u_0$, for the apparatus described. For curves A, $u = 0.0920c$, $\alpha = 4.2$, $I = 8.0 \text{ A}$, $\Omega/\gamma c = 1.10 \text{ cm}^{-1}$ (i.e., $V = 45.8 \text{ kV}$, $B = 2.043 \text{ kG}$); for curves B, $u = 0.0920c$, $\alpha = 5.0$, $I = 8.0 \text{ A}$, $\Omega/\gamma c = 1.17 \text{ cm}^{-1}$ (i.e., $V = 67.6 \text{ kV}$, $B = 2.259 \text{ kG}$). [Note: $f \text{ (GHz)} = 4.775(\omega/c) \text{ (cm}^{-1}\text{).}$]

rent was measured with an integrating current transformer, and cathode voltage was measured with a compensated capacitive voltage divider.

Before and after cathode activation the entire apparatus was baked at 250 °C for 48 h. System pressure, under continuous turbomolecular pumping, was $\sim 10^{-9}$ Torr with the gun off, and $< 5 \times 10^{-7}$ Torr with the gun under full power. The electron beam was formed and guided along a magnetic field provided by five independently energized solenoid coil systems. Along the 60-cm interaction region a ~ 2 -kG field was adjusted to ± 2 -G uniformity. Three coils around the gun provided the requisite broad field minimum of about 400 G at the cathode surface. Four-place digital measurement of all coil currents was essential for reproducibility.

Electronic gain was measured for this apparatus by injecting cw power at each frequency of inter-

est and then inserting whatever series attenuation was required to return the fast-rise-time output crystal-detector voltage to its value with the electron beam off. This method of measurement is independent of the detector linearity and is limited in accuracy only by the calibration accuracy of the attenuators used. Calibrated attenuators were placed in both the input and output guides to insure both linearity and absence of spurious oscillations.

A detailed small-signal theory has been developed for spatial amplification on axisymmetric wave guides penetrated by tenuous electron beams in a uniform magnetic field.⁹ This theory applies to dielectric-loaded waveguides supporting TE_{0n} , TM_{0n} , and EH_{mn} modes and to empty waveguides with finite wall conductivity supporting TE_{mn} and TM_{mn} modes. The theory allows arbitrary input and output boundary conditions to be specified, so that the so-called input coupling loss arising from division of the input signal amongst several copropagating modes in an amplifier is automatically taken into account. Actual beam geometry (i.e., thick annulus, solid beam, radial density profile, etc.) may be included. Finite axial velocity spread is also included, modeled according to the equilibrium distribution function

$$f_0(\gamma, u) = A_s \delta(\gamma - \gamma_0) (\Delta u)^s [(u - u_0)^{2s} + (\Delta u)^{2s}]^{-1},$$

where γ is the total electron energy in units of mc^2 , u is the axial velocity variable, $2\Delta u$ is the full width at half maximum for the distribution, γ_0 and u_0 are constants, A_s is a normalizing constant, and s is a parameter which governs the smear in f_0 : For $s=1$ the distribution is Lorentzian with its extended wings; as $s \rightarrow \infty$ the distribution approaches a box function, zero outside the interval $u_0 \pm \Delta u$. Examples of the predictions of this theory for the geometry of the apparatus described here are shown in Fig. 2(b), in which gain in decibels versus frequency is shown for two different sets of operating conditions (families of curves A and B) and for five values of parallel velocity spread $2\Delta u/u_0$. (The five cases meld together for family A.) The distribution with $s=2$ was chosen for these examples as one which could reasonably approximate that produced by the electron gun used in the experiments. From the dispersion curve [Fig. 2(a)] one can determine that 5.80 GHz is the frequency at which $\omega/k_z = c$; the gain curves of family A are thus for fast waves ($\omega/c < 1.215 \text{ cm}^{-1}$) and those of family B for slow waves ($\omega/c > 1.215 \text{ cm}^{-1}$). As remarked earlier, gain is not predicted at ω/c

$= 1.215 \text{ cm}^{-1}$. Notable in Fig. 2(b) is the sensitivity of gain to velocity spread in the slow-wave region. The examples shown are for conditions of intersection between the dispersion curve and the beam line $\omega = \Omega/\gamma + k_z u$, where $\Omega = eB_z/m$. Two such intersections are shown in Fig. 2(a) for fast- and slow-wave couplings. Examples are not shown here for cases of grazing incidence between dispersion and beam lines, a circumstance known to give rise to slow-wave gain characteristics with wide bandwidth, even for moderate parallel velocity spread.⁵ This is because no substantial gain could in fact be observed for the grazing-incidence condition, a point we shall attempt to explain below.

The experimental results obtained are shown in Fig. 3. Six sets of data (A-F) are given, corresponding to six combinations of gun voltage and magnetic field (values listed in the caption to Fig. 3). Both fast-wave ($f < 5.8 \text{ GHz}$) and slow-wave ($f > 5.8 \text{ GHz}$) interactions were observed, but gain at 5.8 GHz (where $\omega = k_z c$) was not observed, as predicted by theory. Experiments above $\sim 6.6 \text{ GHz}$ could not be performed, because of limits on the magnet power supplies; the tuning width in the slow-wave region is thus greater than the 700 MHz shown in Fig. 3, i.e., greater than 11%. The instantaneous -3 dB bandwidth for curve D is 220 MHz, or 3.7%, at a peak gain of 32 dB. In the fast-wave region (curve A) a bandwidth of 150 MHz, or 2.7%, was observed at a peak gain of about 30 dB. These values compare favorably with gain and bandwidth values reported⁶ for fast-wave gyro traveling-wave amplifiers, i.e., 24 dB and 1.4%.

It remains to explain why the anticipated wide-

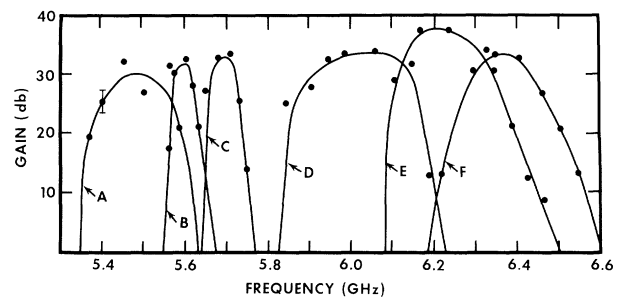


FIG. 3. Measured electronic gain vs frequency for six values of cathode voltage [$-V$ (kV)] and axial magnetic field [B_z (kG)]. A: $V=34$, $B_z=1.90$; B: $V=39.7$, $B_z=1.95$; C: $V=39.7$, $B_z=2.00$; D: $V=42.0$, $B_z=2.06$; E: $V=42.0$, $B_z=2.12$; F: $V=45.4$, $B_z=2.17$. For all cases $I=5 \text{ A}$. Solid curves connect measured points. Typical error bar is shown.

bandwidth values ($\sim 20\%$) were not observed in the slow-wave region. The conditions for wide bandwidth require grazing incidence between beam and guide lines (cf. Fig. 2). For this to be possible for the dispersion curve shown would have required a lower magnetic field (1.9 kG) and a higher slope, corresponding to $\alpha = 2$, $V = 60$ kV. But with $\alpha = 2$, our theoretical calculations indicate that beam velocity-spread values higher than 5% will severely degrade the gain; for the gun available the momentum spread, although not measured, was probably higher than 5%.¹⁰ Thus to observe gain in the presence of large velocity spread evidently required higher α values, making the grazing condition inaccessible in these experiments. For intersecting conditions, such as those shown in Fig. 2(a), higher values of α result; gain can then occur even for large velocity spread. Beyond these qualitative points, a more detailed comparison between theory and experiment is probably not justified since the actual distribution function $f_0(\gamma, u)$ was not known.

In a subsequent experiment, the apparatus was arranged as a feedback amplifier, with a portion of the output signal returned to the input. With suitable phase adjustment, this arrangement allowed effective gain values as high as 53 dB to be observed at 6.2 GHz. Self-sustained oscillations did not occur since the gun voltage pulse did not remain at the gain condition for more than about 50 nsec. Under this high-gain condition, the amplifier power output was 20 kW, corresponding to an electronic efficiency of 10%.

Important discussions with B. Arfin, J. M. Baird, L. R. Barnett, P. Ferguson, A. Ginzburg, and V. L. Granatstein are gratefully acknowl-

edged. Important technical support was provided by R. Downing, J. H. Kearney, R. C. Lee, S. Swiadek, P. Trosuk, and G. Vogel. Assistance with computation was provided by Q. F. Li. This research was sponsored in part by the U. S. Office of Naval Research.

^(a)Present address: Weizmann Institute of Science, Rehovot 76100, Israel.

^(b)Present address: Omega-P, Inc., 2008 Yale Station, New Haven, Conn. 06520.

¹Y. Y. Lau, K. R. Chu, L. R. Barnett, and V. L. Granatstein, *Int. J. Infrared Millimeter Waves* **2**, 373 (1981).

²J. L. Seftor, V. L. Granatstein, K. R. Chu, and M. E. Read, *IEEE J. Quantum Electron.* **15**, 848 (1979).

³J. L. Hirshfield, in *Infrared and Millimeter Waves*, edited by K. J. Button (Academic, New York, 1979), Vol. 1, pp. 1-54.

⁴K. R. Chu and J. L. Hirshfield, *Phys. Fluids* **21**, 461 (1978).

⁵K. R. Chu, A. K. Ganguly, V. L. Granatstein, J. L. Hirshfield, S. Y. Park, and J. M. Baird, *Int. J. Electron.* **51**, 493 (1981).

⁶L. R. Barnett, K. R. Chu, J. M. Baird, V. L. Granatstein, and A. T. Drobot, *IEEE International Electron Devices Meeting Technical Digest* (IEEE, New York, 1979), pp. 164-167.

⁷Type VUW-8080, Varian Assoc. Inc., Palo Alto, Cal. 94303.

⁸*Pulse Generators*, edited by G. N. Glasoe and J. V. Lebacqz (McGraw-Hill, New York, 1948), pp. 152-165.

⁹S. Y. Park, J. M. Baird, and J. L. Hirshfield, B-K Dynamics Technical Report No. TR-3-481, 1982 (to be published).

¹⁰An independent particle simulation to determine beam parameters for this gun was performed by N. Dionne (unpublished). He found a rms parallel momentum spread of 11% with $\alpha = 1.1$ at 42 kV.